Journal of Hazardous Materials B125 (2005) 130–140

Journal of Hazardous Materials

www.elsevier.com/locate/jhazmat

Electro-kinetic dewatering of oily sludges

Lin Yang, George Nakhla*, Amarjeet Bassi

Department of Chemical & Biochemical Engineering, The University of Western Ontario, London, Ont., Canada N6A 5B9

Received 4 March 2005; received in revised form 10 May 2005; accepted 12 May 2005
Available online 6 July 2005

Abstract

An oily sludge from a rendering facility was treated using electro-kinetic (EK) techniques employing two different experimental designs. The bench scale used vertical electrodes under different operational conditions, i.e. varied electrode spacing at 4, 6 and 8 cm with electric potential of 10, 20 and 30 V, respectively. The highest water removal efficiency (56.3%) at bench scale was achieved at a 4 cm spacing and 30 V. Comparison of the water removal efficiency (51.9%) achieved at the 20 V at 4 cm spacing showed that power consumption at 30 V was 1.5 times larger than that at 20 V, suggesting a further increase of electric potential is unnecessary. The solids content increased from an initial 5 to 11.5 and 14.1% for 20 and 30 V, respectively. The removal of oil and grease (O&G) was not significant at this experimental design. Another larger scale experiment using a pair of horizontal electrodes in a cylinder with 15 cm i.d. was conducted at 60 V at an initial spacing of 22 cm. More than 40.0% of water was removed and a very efficient oil separation from the sludge was achieved indicating the viability of electro-kinetic recovery of oil from industrial sludge.

Keywords: Sludge; Electro-osmosis; Dewatering efficiency; Moisture content; Oil and grease

1. Introduction

The ever-increasing demand of industrial products has resulted in more wastes discharged to the natural environment. While the so-called wastes may still contain useful resources, the nature of the contaminants and the waste volume have a detrimental impact on the ecological or social environment. Since water contributes the majority of the volume (or weight) of most industrial wastes, traditional dewatering technologies, such as belt pressing, pressure pressing, centrifugation, sludge drying bed and lagoons focus on removing water from the wastes, but resource recovery is often ignored in these processes. Hence, the necessity of developing a technology to achieve both dewatering and resource recovery is obvious.

Electro-kinetic methods utilize a low-intensity direct current across an electrode pair on each side of a porous medium, causing electro-osmosis of the aqueous phase, migration of ions and electrophoresis of charged particles in the colloidal system to the respective electrode, which depends on the charge of ions and particles [1]. Electro-osmosis is the movement of the capillary water under the electric field due to the existence of the electrical double layer at the interface of water and the solid surface, while electrophoresis is the migration of charged particles or ions in a colloidal system towards the counter charged electrode. The direction of the electro-osmotic flow is decided by the nature of the charges on the surface of solid particles, i.e. negatively charged particles resulting in water going towards cathode while positively charged particles making water move towards anode.

This developing technology has been proven to be effective not only in dewatering and the removal of soluble ions and neutral organics, but also in the removal of insoluble organics in the porous media [1–10]. Research on sludge dewatering and soil remediation from heavy metal and organic contamination has been performed for many years. Raats et al. [2] reported an increase in solids contents from 17 to 24% in drinking water sludge by incorporating

* Corresponding author. Tel.: +1 519 661 2111; fax: +1 519 850 2921.
E-mail address: gnakhla@eng.uwo.ca (G. Nakhla).

0304-3894/$ – see front matter
doi:10.1016/j.jhazmat.2005.05.040

electro-kinetic dewatering in a gravity-driven thickening belt combining with a belt press in a full-scale experiment with additional energy consumption of 60 kWh/t of sludge. Yuan and Weng [3] also achieved a high water content reduction from 87.8 to 62.6% in municipal sludge at a potential gradient 5.0 V/cm in 41 h using a 6 cm long electro-kinetic dewatering cell. Electro-osmosis and electrophoresis are the two most important mechanisms for water removal and the improvement of cake building in sludge dewatering processes [6]. Besides the sludge dewatering investigations, electro-kinetic remediation of soil using either vertical [7] or horizontal-electrodes [8] implanted in the soil was studied as well. Removal of higher than 90% of the metals was observed by an improved electro-kinetic process employing a cation selective membrane in front of cathode to prevent the precipitation of metals in the vicinity of cathode [9]. Cundy and Hopkinson [10] showed a prospect application of in situ electro-kinetic decontamination and consolidation of soil with ferric iron remediation and stabilization technique.

Research on electro-kinetic removal of neutral soluble or insoluble organic compounds from soil showed encouraging results as well [5,8]. Maini et al. [5] reported greater than 90% removal of hydrophobic polycyclic aromatic hydrocarbons (PAHs) by electro-kinetics in bench- and pilot-scale experiments, while in another study, Ho et al. [8] reported 98% removal efficiency of *p*-nitrophenol in one pilot unit. Electro-kinetic remediation organic contaminants in soil has been proven to be promising, and the experimental results from the above studies [5,8] suggest the possibility of transporting hydrophobic neutral molecules (such as oil) from a porous medium, i.e. industrial wastes by electro-osmotic flow.

Oil, a group of hydrophobic hydrocarbons, is not only a contaminant in the natural environment but also a reusable resource. The research group at Concordia University, Que., Canada, has performed investigations on phase separation in petroleum industrial sludges and they attribute the separation of diesel from its suspensions to electro-kinetic phenomena [11]. The application of electro-kinetic treatment technology for the oily sludge/wastes in other industries is scarce and very limited information in this respect has been reported in the literature.

Oily sludges can be generated in many industries, such as food processing and mechanical manufacturing, among others. The food processing, especially meat processing and edible oil manufacturing industry produce huge quantities of oily sludges. In this study, dissolved air floatation (DAF) sludges, which consists of meat protein particles and oil and grease (O&G) from a rendering facility, were treated by the electro-kinetic method. The objectives of this research were to investigate the effect of electro-kinetic processes on the removal of water and oil from the sludge as well as the influence of the strength of the electric field and the electrode spacing on the separation of oil and sludge dewaterability.

Table 1
Composition and properties of the sludge

Composition	
Water content	66–79 wt.%
O&G content	16–30 wt.%
Total solids	3–7 wt.% (chicken meat particles)
Volatile solid	>95% of total solids
Properties	
pH	5.3–5.6
Density (kg/L)	0.95
Specific gravity of solids (kg/L)	0.90
Specific heat capacity	
Oil (kJ/kg °C)	2.1
Water (kJ/kg °C)	4.2
Solids (kJ/kg °C)	3.0
Particle size (μm)	10–50
Zeta potential (mV)	1.41
Isoelectric point of sludge particles (pH)	5.9

2. Materials and experimental method

2.1. Sludge

The sludge was provided by a pet food industry in the province of Ont., Canada. It should be mentioned that the wastewater has been treated on-site by a two-stage oil recovery system upstream of the DAF. The composition of the solid particles is primarily protein from chicken meat, and ground chicken bones. Detailed characteristics of the sludge used in this experiment are listed in Table 1.

2.2. Experimental setups

A series of bench-scale experiments were conducted in the electro-kinetic dewatering cell shown in Fig. 1a. The dimensions of the cell were 14 cm (L) × 10 cm (W) ×10 cm (H). The cell was made of PVC and the anode was a slotted graphite sheet with an opening size of 1.3 mm per slot, while the cathode was a stainless steel mesh. Two pieces of fibreglass filter papers (Whatman No. 42) were attached on both inner sides of the anode and the cathode to retain solids. The filtrate was removed by a pipette periodically during the 3-h dewatering processes. Another larger scale setup (Fig. 1b) with horizontal-electrodes (a movable top graphite anode and a fixed bottom porous stainless steel cathode) was operated in a batch mode with 4 L of the same sludge to investigate the efficacy of EK method in an enlarged scale with 60 V electric field. The inside diameter of the cylinder was 15 cm and the initial height of the sludge was 22 cm. In order to truly delineate the impact of electro-kinetic dewatering (EKD) at each experimental condition, controls without electricity were employed. All experiments were conducted at room temperature, i.e. 20–22 °C.

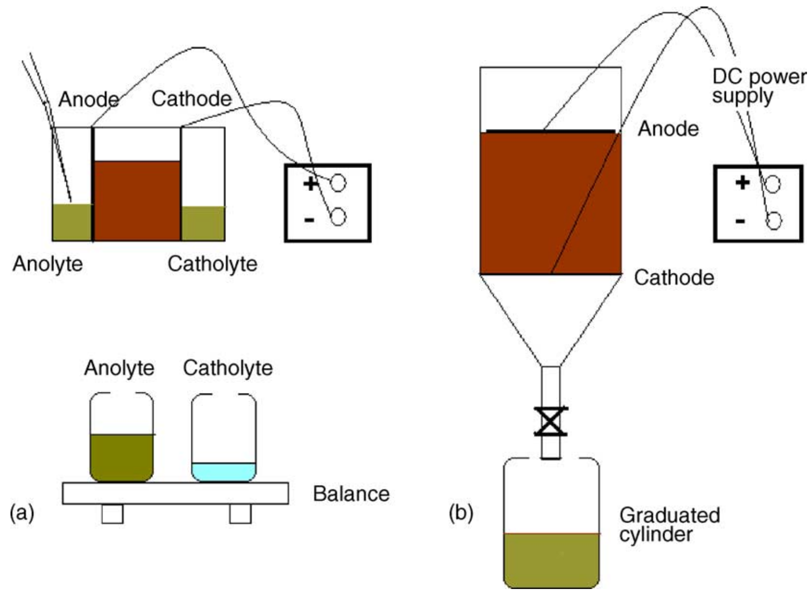

Fig. 1. Experimental setups.

2.3. Experimental design

In the bench-scale system, three different voltages were used, i.e. 10, 20 and 30 V. Several potential gradients in the range of 1.7–7.5 V/cm were examined. Two to five experimental runs were repeated to ensure reproducibility. The cumulative weight of filtrate (including oil extracted from the sludge) as well as variations of the electric current, potential and pH distribution in the process of the experiment was monitored and recorded. After 3 h, the cell was disconnected from the DC power supply and sludge samples were taken at different positions between the two electrodes to measure the moisture and O&G contents, and the concentrations of O&G in the filtrate were measured as well.

In the larger scale system, a constant voltage of 60 V throughout the experiment was tested. To assess the impact of heat generation, another experimental run was started initially at 60 V, followed by disconnection from the power as well as re-connection to 30 and 15 V. The monitored parameters in the process of the experiment included: cumulative weight of the filtrate, electric current and temperature. The moisture and O&G contents in both the raw and treated sludge were measured after the experiment.

2.4. Analytical methods

The analyses of O&G in the filtrate and treated sludge were carried out by the standard gravimetric method [12]. This method uses hexane as the solvent to extract O&G out of the aqueous sample to a known weight empty boiling flask, evaporating the solvent and measuring the weight of the flask after the evaporation. The weight gain of the flask was divided by the volume of the sample to calculate the concentration of O&G.

The sludge samples were heated at 105 °C for 24 h to remove all the moisture. The loss of the weight of the sludge sample after heating is the weight of the moisture. The value of moisture content is equal to the ratio loss of weight to the initial weight of the sludge samples.

Zeta potential was measured by the zeta potential analyzer mode Zeta Plus, manufactured by Brokhaven Instrument Corp. The Zeta Plus is used to measure a suspension with particles ranging from a few nanometers to as large as 30 μm diameter. It uses electrophoretic light scattering and the laser doppler velocimetry (LDV) method to determine particle velocity, and from this, the zeta potential. Before measurement, the analyzer's accuracy was checked the by a standard suspension provided by Brokhaven Instrument Corp. Seven samples with pH of 2.3, 3.7, 4.1, 5.6, 6.6, 7.1 and 8.33 were used to determine the isoelectric point and zeta potential of the raw sludge. For each pH, three identical samples were tested and readings were repeated for six times in each sample. The average values were used to determine the zeta potential listed in Table 1 and the variation of zeta potential versus pH is presented in Fig. 2.

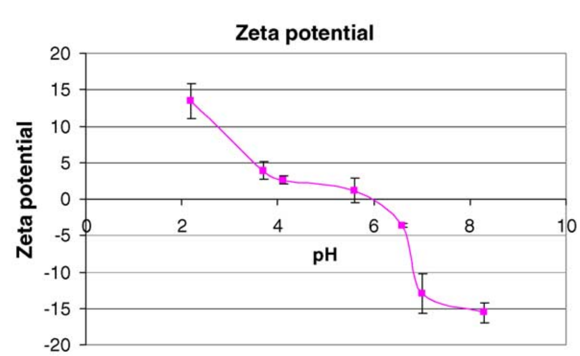

Fig. 2. Zeta potential.

Specific resistance to filtration was measured using a standard Buchner funnel. About 200 g of sludge was vacuum filtered at a vacuum pressure of −70 kPa. The volume of the filtrate was monitored as a function of time. The graph of filtration time/filtrate volume versus filtrate volume was drawn according to the experimental data and the slope of the curve represents the magnitude of the resistance to filtration [13].

3. Experimental results and discussion

3.1. Bench scale

3.1.1. Dewatering efficiency

The effect of EKD on dewatering efficiency was presented in Table 2. In the context of this paper, dewatering efficiency refers to the ratio of the filtrate weight to the initial weight of water in the sludge, i.e. the percentage of raw sludge water collected in the filtrate on a weight basis. In the present study, the occurrence of two electro-osmotic flows, namely anolyte and catholyte as shown in Table 2, corresponding to the respective movements toward either the anode or cathode, was observed in all experiments. This phenomenon was intensified by the fact that both of the two flows increased with the increase of the electric potential on the two sides of the electrodes though the most obvious one occurred at the 4 cm electrode spacing. It is interesting to note that Yuan and Weng [3] observed only catholyte during dewatering of municipal sludge cake and similarly Habibi [11] also observed the movement of liquid toward cathode during electro-kinetic dewatering of oily sludge from a crude oil storage tank. Since the pH of the sludge is lower than its isoelectric point of 5.9, meaning positive charges on sludge particles predominate, most of the electro-osmotic flow was towards the anode. The occurrence of the catholyte suggested negatively charged particles were also present in the sludge since the nature of the charge on the surface of the solid particles governs the direction of the electro-osmotic flow (while positively charged particles dominated in the suspension).

The dewatering efficiency at the 4 cm electrode spacing in 3 h was very pronounced. More than 50% of water was removed when the electric potential gradient was larger than 5 V/cm. Dewatering efficiency decreased with increasing electrode spacing even though the potential gradient across the electrodes were the same, i.e. 10 V at 4 cm electrode spacing and 20 V at 8 cm electrode spacing. The reason for this phenomenon was that the effective potential, which was exactly applied on the two sides of the sludge was different since the potential losses at the interfaces between the sludge and the two electrodes were different under the two conditions. For example, under the condition of 10 V and 4 cm, the measured effective potential was about 5.7 V which translates into an effective potential gradient about 1.7 V/cm (the thickness of the sludge cake was considered as 3.4 considering 0.3 cm thickness of sludge-electrode interfaces), while under 20 V and 8 cm, the measured effective potential was 9.5 V giving rise to a potential gradient of about 1.3 V/cm. This suggests that small electrode spacing can better benefit the sludge dewatering processes.

By comparing the dewatering efficiency at 20 and 30 V, evidently as shown in Table 2, the impact of applied voltage on dewatering efficiency followed the rule of diminishing returns. This means that the biggest improvement occurred upon the increase of voltage from 10 to 20 V while further increase to 30 V affected only a marginal improvement. Dewatering efficiency changed from 51.9 to 56.9% at 4 cm electrode spacing, from 42 to 40% at 6 cm spacing and from

Table 2
Dewatering efficiency of EKD

Experimental conditions	Anolyte (g)	Catholyte (g)	Total weight of filtrate (g)	Dewatering efficiency (%)		Potential Gradient (V/cm)	Power consumption (WH/100 g of sludge)
				Total	Net		
At 4 cm							
10 V (3)	20.0 ± 3.2	11.0 ± 1.8	30.5 ± 4.5	41.3	14.1	2.5	4.0
20 V (3)	26.4 ± 1.8	12.5 ± 1.6	38.9 ± 3.1	51.9	24.7	5	8.3
30 V (3)	29.0 ± 1.7	13.2 ± 3.8	42.2 ± 2.9	56.3	29.1	7.5	12.4
Control (0 V) (6)	11.4 ± 0.2	9.0 ± 0.3	20.4 ± 0.4	27.2		0	0
At 6 cm							
10 V (3)	12.9 ± 0.7	8.4 ± 0.0	21.3 ± 1.0	28.4	2.4	1.7	4.6
20 V (5)	20.8 ± 1.0	10.8 ± 1.0	31.6 ± 1.9	42.1	16.1	3.3	13.6
30 V (3)	20.3 ± 0.9	9.6 ± 0.2	29.9 ± 1.5	39.9	13.9	5	15.1
Control (0 V) (10)	10.3 ± 0.6	9.2 ± 1.2	19.5 ± 1.5	26.0		0	0
At 8 cm							
20 V (2)	17.8 ± 0.5	7.6 ± 0.3	25.2 ± 0.2	33.6	11.3	2.5	13.5
30 V (3)	18.3 ± 0.2	8.2 ± 0.0	26.5 ± 0.2	35.3	13.0	3.8	20.3
Control (0 V) (4)	9.4 ± 0.6	7.4 ± 0.3	16.7 ± 0.7	22.3		0	0

Note: Dewatering efficiency = weight of total filtrate/intial weight of water in the sluge (take the initial moisture content as 75%). The data in the table were based on 100 g of sludge. Net dewatering efficiency is the total dewatering efficiency (left) minus the efficiency of the control (without electricity). Numbers within parenthesis in the first column indicate the no. of replicates.

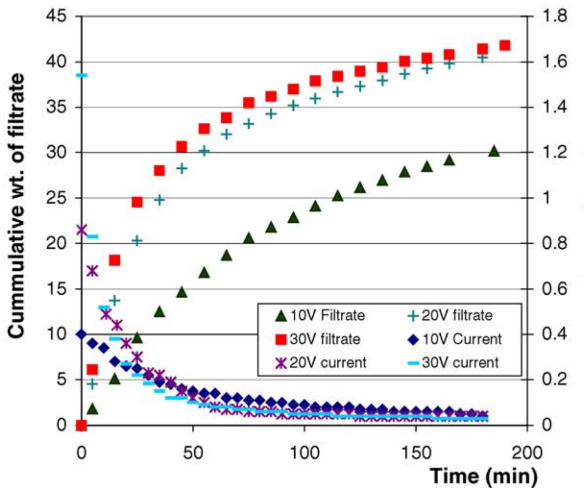

Fig. 3. Current and weight of filtrate vs. time at 4 cm electrode spacing.

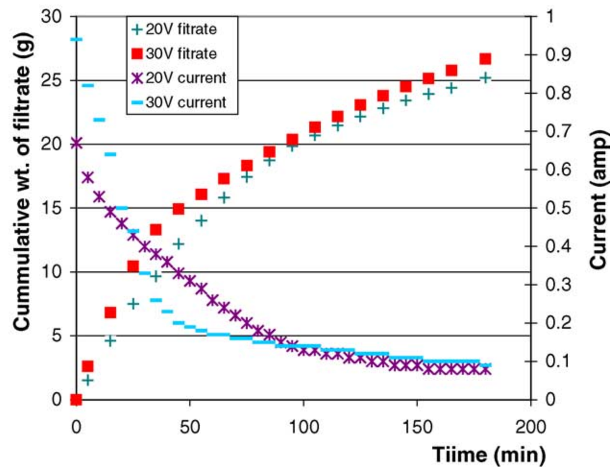

Fig. 5. Current and weight of filtrate vs. time at 8 cm electrode spacing.

33.6 to 35.3% at 8 cm spacing, despite a much higher power consumption.

The cumulative filtrate weight and variation of current throughout the 3-h experiments for the three electrode spacings, i.e. 4, 6 and 8 cm are depicted in Figs. 3–5, respectively. All experiments conformed to a general trend of rapidly decreasing current concurrent with a sharp increase in filtrate volume. During the EKD processes, as shown in Figs. 3–5, the initial 40 min were very critical for process efficiency, since both the current and the filtrate flow rate peaked at the beginning. As the water and ions were transported to the filtrate compartments at much higher rate in the beginning, the total electric resistance increased markedly causing a sharp current decrease followed by a sharp reduction of electro-osmotic flow. The rate of electro-osmotic flow reached a relatively constant value irrespective of the applied potential differences, indicated by the almost parallel curves of cumulative weight of filtrates versus time.

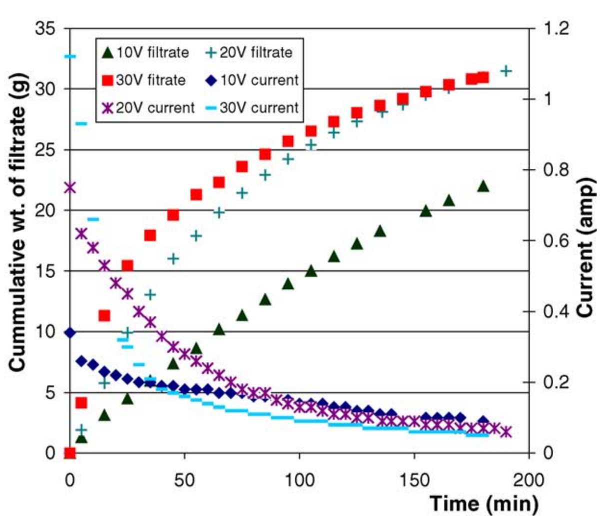

Fig. 4. Current and weight of filtrate vs. time at 6 cm electrode spacing.

3.1.2. Dewaterability

Specific resistance to filtration (SRF) was used to evaluate the dewaterability of sludge at 1 and 2-h contact times. Fig. 6a and b shows, respectively, the results of the 1-h vacuum filtration (VF) and EKD experiments, while Fig. 7 shows the 2-h tests results. The slopes of the time/volume versus volume depicted in Figs. 6 and 7 represent SRF with the connotation that the larger the slope the greater is the resistance to filtration. All the slopes of the triplicates runs for the VF experiments, both at the 1 and 2-h contact times, varied very narrowly from 0.0164 to 0.0174 min/mL^2 highlighting the reproducibility and accuracy of the requirement results. It is evident, from Figs. 6a and b that the SRFs in EKD during the first 1-h were lower than VF. However, in the 2-h experiment, while the initial dewaterability of EKD process was better than VF, the overall resistance to filtration in 2-h EKD at 10 V readily exceeded the VF, with the SRF at 30 V same as VF. It should be noted that the value of SRF at 30 V was unexpected since it was higher than at 20 V due to a much faster filtrate flow rate in the first 25 min at 30 V relative to that of 10 and 20 V, followed by a precipitous drop afterwards. As shown in Fig. 8, the curve of dQ/dt versus time at 30 V was much steeper than the others. Thus, SRF started to increase after 25 min and resulted in the increase in the final SRF.

3.1.3. Removal of O&G

The quantity of oil and grease removed from the sludge into the filtrate was concentrated in the anolyte as compared to the catholyte. This is advantageous to the catholyte-dominated electro-osmotic processes occurring in most other applications, since it eliminates the potential reactions between highly concentrated hydroxyl ions within the cathode area and O&G resulting in the formation of soap which is undesirable for oil recovery.

Thorough analyses of O&G in both anolyte and catholyte, the O&G distribution in the sludge bed and the mass

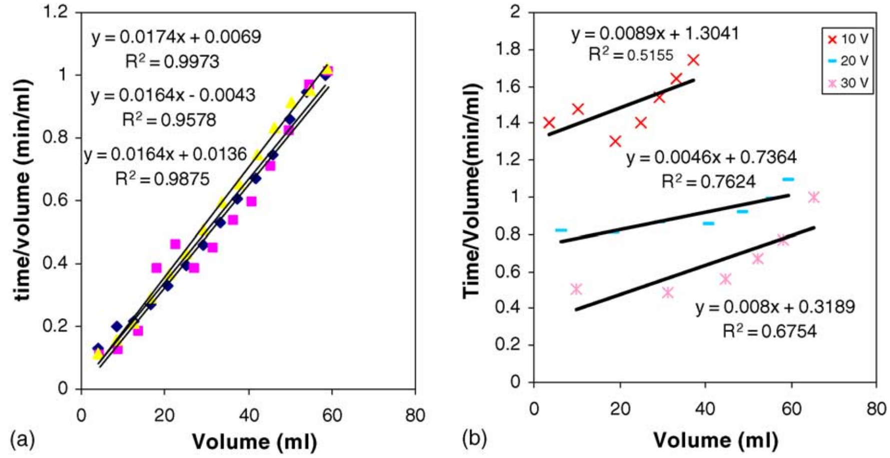

Fig. 6. Specific resistance to filtration at 1 h of operation: (a) vacuum filtration and (b) EKD.

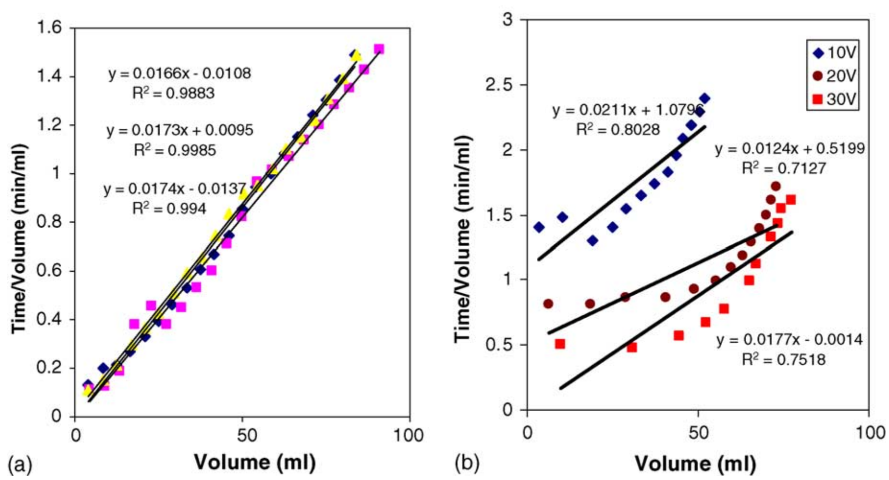

Fig. 7. Specific resistance to filtration at 2 h of operation: (a) vacuum filtration and (b) EKD.

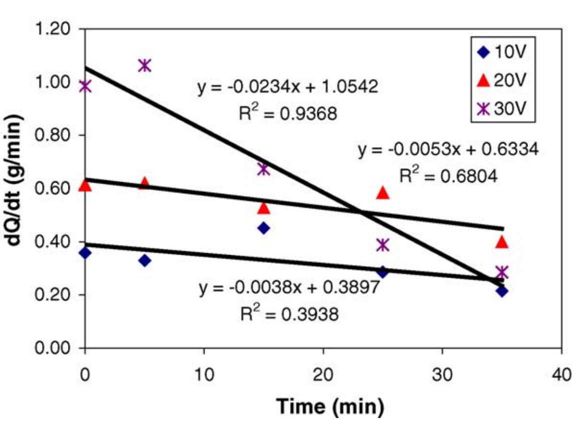

Fig. 8. Flow rate of filtrate vs. time.

balance are presented in Tables 3 and 4. As apparent from Tables 3 and 4, the removal of O&G from the sludge into the filtrate increased with the increase of applied electric potential. At 10 V and 4 cm electrode spacing, as we can see from Table 3, O&G concentrations in the filtrates were much lower than those under 20 V and 6 cm spacing, even though the dewatering efficiencies under the two conditions were pretty close, i.e. 41.3 and 42.1%, respectively. The highest O&G concentration in the filtrates was obtained at a 8 cm spacing and 30 V, but the dewatering efficiency of 35.3% was lower than those under the above two conditions. However, from Table 4, we can see the difference of the percentage of oil removal from the raw sludge on a mass basis between all spacings, is not significant since less filtrate volumes could be achieved at the wider spacing. This clearly shows that while oil recovery is not adversely impacted by electrode spacing, dewatering efficiency is.

Table 3
O&G distributions

Samples	Filtrate (g/L)		Sludge (wt.%)					
	Anolyte	Catholyte	Anode		Middle		Cathode	
			O&G	Moisture	O&G	Moisture	O&G	Moisture
4 cm, 10 V	0.68	0.11	38.8	49.0	31.6	58.2	26.5	65.2
4 cm, 20 V	5.78	0.65	41.6	43.9	29.8	59.9	27.9	62.4
6 cm, 20 V	2.4	0.8	42.0	45.9	27.0	65.6	26.8	65.7
8 cm, 20 V	8.46	0.78	41.7	43.8	18.4	76.8	23.3	70.2
4 cm, 30 V			44.4	37.3	30.7	56.7	27.8	60.8
6 cm, 30 V	25.04	2.14	43.8	46.9	28.5	67.4	28.8	67.9
8 cm, 30 V	49.9	3.38	44.6	35.5	14.9	78.5	21.1	69.2

Table 4
Oil and grease mass balance

Experimenta condition	Average O&G in final Sludge (%)	Water removed (mL)	Final sludge mass (g)	Oil in final sludge (g)	Oil removed in filtrate (g)	Average O&G in raw sludge (%)
4 cm, 10 V	32.4	30.5	69.0	22.4	0.015	20.6
4 cm, 20 V	33.1	38.9	61.1	20.2	0.16	
8 cm, 20 V	27.8	25.2	74.6	20.7	0.16	
4 cm, 30 V	34.3	42.2	57.8	19.8		
6 cm, 30 V	33.7	29.9	70.1	23.6	0.53	
8 cm, 30 V	26.9	26.6	73.5	19.8	0.94	

The mass balance calculation was based on 100 g raw sludge; The average O&G concentration taken from the average values of the three concentrations at anode, middle, and cathode area of the sludge bed, which caused the error in mass balance.

By monitoring the current variations as a function of time during the EKD processes under different conditions, the bigger volumes of sludge obtained at larger electrode spacing could better maintain the current at a higher level than the smaller volumes. For example, at 30 V, the current was around 0.03 A after 1.5 h at 4 cm spacing while at 8 cm spacing the current was three times larger till the end of experiments. The time for observation of oil in the anolyte, for example, at 8 cm electrode spacing was 100 min at 20 V as compared to 80 min at 30 V, and the electro-osmotic mass flow rates decreased from 1.0 to 0.24 g/min at 100 min at 20 V and from 1.4 to 0.27 g/min at 80 min at 30 V. This demonstrates that at the high filtrate flow rate at the beginning of the EKD process, no free oil could pass through the filter, and hence oil accumulated at the anode area where a layer of liquid O&G could be observed. Much higher concentrations of O&G in sludge samples taken from the anode area also confirmed that the oil migrated with the electro-osmotic flow towards the anode and accumulated there. One of the possible explanations for this is that the relatively larger molecular size (20 Å of oil [14] and 3.0 Å of water [15]) and much higher viscosity of O&G (27.7 mm^2/s for chicken fat [16] and 41.2 mm^2/s for oleic acid [17] at 38 °C versus 0.658 mm^2/s [18] for water at 40 °C) could not favorably compete with water molecules to pass through the filter (inside the two electrodes) at the same rate. Once the water flow rate declined, more pores of the filter paper were available for O&G to pass through. This substantiates the viability of O&G removal by the application of electrical field. In order to verify this observed lack of competitiveness of oil and grease with water in electro-osmosis flow towards the anode, another bench-scale experiment was performed with gravity pre-thickened sludge. In this experiment, O&G was driven out of the sludge to the filtrates as soon as the electricity was connected with the initial anolyte and catholyte mass flow rates of 0.16 and of 0.1 g/min, respectively. Both anolyte and catholyte contained approximately 1:1 water and O&G by volume after 3 h of treatment, as shown in Fig. 9.

The other hypothesized mechanism for the oil movement, elaborated upon here, is driven by the increase in sludge pH. Fig. 10 shows the distribution of pH at different locations in the sludge bed at different electrode spacings. The reproducibility of the results is highlighted by the almost identical

Fig. 9. Anolyte (right) and catholyte (left) of the EKD of gravity pre-thickened sludge.

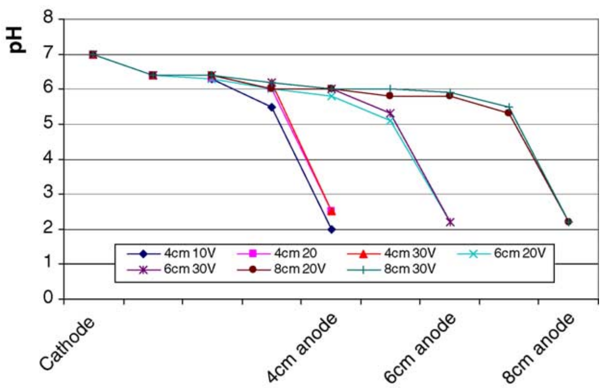

Fig. 10. pH and temperature distribution during EKD processes.

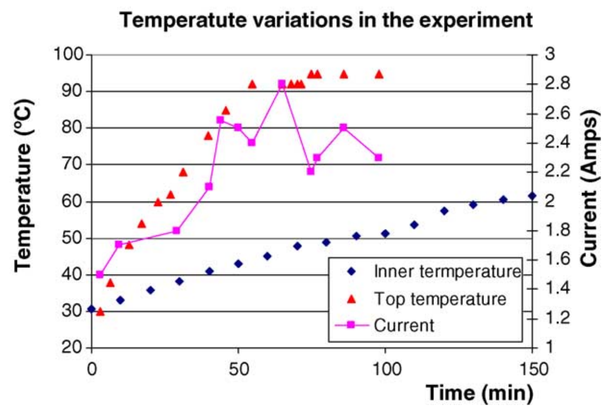

Fig. 11. Temperature and current profiles in the larger scale experiments.

pH profile for the duplicates at various voltages. As soon as the cell was connected to the DC power supply, the distribution of pH along the length of the sludge was increased from around 5.4 to above 6.0 except for the interface of sludge and anode. The increase of pH was due to the transportation of hydroxyl ions—the product of electrolysis of water at the cathode by the anolyte towards the anode. The increased pH can enhance the dissociation of fatty acid in the sludge into negatively charged fatty acid $RCOO^-$ radicals and H^+. The generated H^+ and OH^- formed water in the sludge, and forced the reaction towards dissociation. $RCOO^-$ might combine with metal ions, such as Na^+ and K^+ presented in the sludge to form the fatty acid salt which is a type of a surface-active agent. The formation of the surfactant can help displace oil from the surface of solid into the aqueous phase by changing surface electric charges due to adsorption and interfacial tension [19]. Moreover, the extra negatively charged fatty acids radicals $RCOO^-$, which did not react with the limited metal ions could migrate to the anode by electrostatic forces and recombine with H^+ at the extremely acid environment in the anode area where the pH was around 2.

3.2. Dewatering and oil recovery in the larger scale experiment

Two larger scale EKD experiments were conducted using horizontal-electrodes design, in which 4 L of sludge with an initial height of 22 cm were used. In the first experiment, a constant 60 V was used, while in the second, the initial voltage of 60 V was applied for 1 h and then followed by disconnection with the power supply for 30 min, reconnection to 30 V for 10 min, and finally 15 V for 40 min. The results of the experiment are illustrated in Table 5. As apparent from a comparison of the data in Tables 2, 5 and 6, the performance of the larger scale was much better than that of the bench scale one.

The temporal current and temperature profiles in this experiment are depicted in Fig. 11. Comparing Figs. 3–5 and Fig. 11, the current in the larger scale EKD cylinder increased as opposed to the bench-scale cell where it decreased. As already discussed above, the electro-osmotic flow in this sludge moves towards the anode. The downward movement of water by gravity was hindered by the upward electric force

Table 5
Experimental results from horizontal-electrode setup

Experiment 1[a]											
Time (min)	0			20			90			120	
Current (A)	1.3			1.3			2.3			2.8	
Volume (mL)											
Water							200			1400	
Oil										800	
Sludge										1300	
Experiment 2[b]											
Potential (V)	60	0	30	15							
Time (min)	0	20	40	46	51	56	62	70	85	95–105	145
Current (A)	1.8	1.9	3.4	3.5	4.0	0	0	0	0	1.8	0.8
Volume (mL)											
Water				200	300	400	500	600	700	720	1000
Oil											400
Sludge											2100
Moisture and O&G content in final sludge						45.8% moisture, 32.4% O&G					

[a] 120-min EKD at constant voltage 60 V, initial sludge volume of 4 L.
[b] 145-min EKD at varied voltages from 60 to 0 V, initial sludge volume of 4 L.

and as a result the electric resistance of the sludge and the current could be maintained. The higher electric current generated a large amount of heat, sufficient to rapidly increase the inside temperature in a short time. This decreased the electric resistance of the electrolyte, which in turn increased the electric current and ultimately the temperature. The biggest potential loss in the experiments was observed at the interface of sludge and the graphite anode, consistent with the findings of Mohamedelhassan and Shang [20], who attributed this to the electrochemical potential of the electrode material. Materials with low-electrochemical potential have a low-electrode/electrolyte interface voltage loss. The electrochemical potential of iron (cathode) is −0.44 V while carbon (anode) is +1.18 V, and accordingly larger voltage loss occurred at the interface of the anode and the sludge. As a result more heat is generated in the anode area, thus increasing the local temperature. Consequently, the temperature at the anode (top) was higher throughout the experiments. The inner temperature gradually increased from a room temperature of 30 °C to a relatively equalized temperature of 60 °C inside the sludge bed except for the anode area. The variation of current and temperature (monitored on the top and at the center of the sludge bed) is demonstrated in Fig. 11.

From the data listed in Table 5, we can see that at the beginning of the operation, the water drained to the bottom at a very low rate. After 40 min when the temperature in the vicinity of the anode reached above 80 °C with inner temperature of about 45 °C, the water drained at a very high speed. Even after disconnection of the cylinder from the power supply, water flow rate was still very high, implying that the separation of water from solids was due to the high temperature in the sludge bed rather than electro-osmosis. The overall weight reduction (reduced weight of sludge/initial weight) in sludges observed in the two experiments of 46.5–68.5% is remarkable. Churaev et al. [21] observed a viscosity reduction with elevated temperature and completely disappearance at about 70 °C in quartz capillary, suggesting that high temperature destroys hydrogen bonded immobile vicinal water surrounding the particles, which helped coagulate particles and liberate more interstitial water, therefore causing the separation of water and solid. In our study, the control setup used to assess temperature and gravity achieved approximately a 25 wt.% reduction without an obvious oil separation.

The separation of oil from solids was believed to be brought by electro-osmosis, which generated a stream of hot water flow moving towards the anode and distributed hydroxyl ions formed at the cathode by the electrolysis of water throughout the sludge bed. As soon as the DC power supply was connected, a thin layer of anolyte mixed with liquid oil droplets floated on top of the anode, which subsequently evaporated by the high temperature of the anode. With time, a layer of oil formed and the thickness increased gradually from a very thin layer to as thick as 2 cm at the end of the experiment. While the exact mechanism for the three-phase separation in this experiment was not explored, the phenomena observed in this EKD process suggested the aforementioned mechanisms.

As described in above section, the formation of surfactant (the salt of fatty acids) displaced oil to the aqueous phase from the surface of the solids particles and the oil could be transported by the upward electro-osmotic flow. Furthermore, observing that the temperature in the dewatering cylinder was much higher than the bench cell, the contribution of the temperature could not be ignored. High temperature is used to recover free oil from the chicken wash water in the plant where the experimental sludge was taken. Research on oil recovery from sand revealed that for rich oil sands, “the rich oil slurry and hot water are all that is needed to release sufficient quantities of natural surfactants into the aqueous phase” [19]. It can be speculated that hot water and the resultant surfactants are the active agents in oil–solid separation in our EKD process. In addition, hot water flow generated by electric current could flush the surfaces of the particles by shear force to tear the oil. Moreover, the resultant surfactants formed a water/oil emulsion, which migrated towards the anode by electro-osmosis. The water subsequently evaporated, leaving oil to float on the top and the evaporated water in turn contributed water removal as well.

3.3. Comparison between the larger scale and bench scale

The moisture content and the concentration of O&G in the final sludge are listed in Table 6. The dewatering and deoiling efficiency was higher than the bench-scale setups in the larger scale. The moisture content in the treated sludge was the lowest (45.8%) in the larger scale compared to the average moisture contents of 51.6–61.1% in the bench scale, while O&G concentrations were close. The high efficiency is believed to be due to the higher temperature in the larger scale system, which facilitated the settlement and evaporation of water and the migration of oil toward the anode due to the decrease in viscosity.

The higher current in the large scale reflects the lower electrical resistance of the system. The resistance of a conductor can be related as follows [22], while the conductivity

Table 6
Comparison of characteristics of the final sludge

Samples		Average moisture (%)	Average O&G (%)	Average solids (%)
Bench scale	4 cm, 10 V	57.3	32.4	10.3
	4 cm, 20 V	55.4	33.1	11.5
	6 cm, 20 V	59.1	31.9	9.0
	8 cm, 20 V	63.6	27.8	8.6
	4 cm, 30 V	51.6	34.3	14.1
	6 cm, 30 V	60.7	33.7	5.6
	8 cm, 30 V	61.1	26.9	12.0
Large scale		45.8	32.4	21.8

is function of temperature [23]:

$$R = \frac{1}{k}\frac{l}{A} \tag{1}$$

$$k_t = k_{25}[1 + 0.02(T - 25)] \tag{2}$$

where k is the conductivity of the electrolyte and T is the temperature in °C; l the distance between the two electrodes and A is the contact surface area of the electrolyte and the electrodes. Using the ambient temperature of 32 °C, a length of 8 cm and a surface area of 45 cm^2 in the bench cell as well as the larger scale average temperature of 45 °C, length of 22 cm and the surface area of 177 cm^2, the electrical resistance in the bench scale was estimated to be 1.8 times larger than the larger scale.

As apparent from the comparison of resistance, in the larger scale, the initial resistance was much lower resulting in higher initial current, thus generating more heat to increase the temperature of the sludge. The loss of water in the larger scale was brought not only by thermal separation and gravity settling, but also by temperature. By conducting a water mass balance based on the initial and final moisture content of the sludge in conjunction with the water collected, it appears that evaporation accounted for about 30% of the water loss in the large scale compared to only 12% in the bench unit.

A detailed energy balance was conducted to assess the contribution of evaporation directly to water loss in the larger scale system. The difference between the input electrical energy of 830 kJ and the energy requirement for heating the sludge of 650 kJ would only be sufficient to evaporation about 80 g of the 500 g of water lost (Table 5). However, the estimation of molecular diffusion from the surface of the sludge indicates the potential for evaporation of 600 g [24] due to the increase in diffusivity of water as a result of the high temperature.

3.4. Summary

The mechanism of water removal in these two scale experimental designs was different. The water removal in the bench-scale system with two vertical electrodes was brought by electro-osmosis of water and the hydraulic pressure in the sludge bed, with the evaporation of water insignificant comparing to the above two effects. In the larger scale experiment, where two horizontal-electrodes were employed, the thermal effects and evaporation due to the high temperature contributed to water removal. The electro-osmotic flow of water towards the upper anode in the larger scale setup, contributed to the movement of oil and the evaporated water.

4. Conclusions

Based on the findings of this study, the following conclusions can be drawn:

- Electro-kinetic dewatering was very effective in reducing the weight of the protein-rich sludge. In our bench-scale experiments, using two vertical electrodes, more than half the water content could be removed with a sufficient electrical field, i.e. 20 V at an electrode spacing of 4 cm. While further increase in the electric field to 30 V, increased dewatering efficiency from 51.9 to 56.3%, the much higher power consumption suggests that at the same scale, a further increase of the strength of electrical field had little effect on water removal efficiency. In the larger scale EKD cylinder which using horizontal-electrodes the water removal was brought by thermal and evaporative effects. The observed dewatering efficiency was 40.0% with final moisture content of 45.8%.
- O&G was removed by the electro-osmotic flow in both experimental designs. In the bench-scale system, filtrates from wider electrode spacing contained higher O&G concentration than smaller spacing, but the percentage oil recovery on a mass basis was independent of the electrode spacing. Water removal efficiency decreased with electrode spacing in the bench-scale system, with the dewatering efficiency at the 8 cm spacing of 35% well below the 56% observed at 4 cm spacing.
- The larger-scale system utilizing the 3.8–4 L of sludge affected significantly better dewatering efficiency and oil recovery than all the bench experiments, with an average weight reduction of sludge of 46.5–68.5%
- The upward anodic electro-osmotic flow in the EKD cylinder with horizontally positioned electrodes has proven to be advantageous in realizing three-phase separation to achieve simultaneous oil recovery and water removal.

Acknowledgements

The financial support for this study, provided by CRESTech (under Grant No. WRPF022) and experimental sludge from Finnie Distributing Inc. are gratefully appreciated.

References

[1] J. Virkutyte, M. Sillanpää, P. Latostenmaa, Electrokinetic soil remediation—critical overview, Sci. Total Environ. 289 (2002) 97–121.
[2] M.H.M. Raats, A.J.G. van Diemen, J. Lave'n, H.N. Stein, Full scale electrokinetic dewatering of waste sludge, Colloids Surf. A: Physicochem. Eng. Aspects 210 (2002) 231–241.
[3] C. Yuan, C. Weng, Sludge dewatering by electrokinetic technique: effect of processing time and potential gradient, Adv. Environ. Res. 7 (2003) 727–732.
[4] K.Y. Lo, K.S. Ho, I.I. Inculet, Electro-osmotic strengthening of soft sensitive clay, Can. Geotech. J. 28 (1991) 62–73.
[5] G. Maini, A.K. Sharman, C.J. Knowles, G. Sunderland, S.A. Jackman, Electrokinetic remediation of metals and organics from histor-

ically contaminated soil, J. Chem. Technol. Biotechnol. 75 (2000) 657–664.
[6] K. Weber, W. Stahl, Improvement of filtration kinetics by pressure electrofiltration, Sep. Purif. Technol. 26 (2002) 69–80.
[7] S.V. Ho, C.J. Athmer, P.W. Sheridan, A. Shapiro, Scale-up aspects of the Lasagna^{TM} process for in situ soil decontamination, J. Hazard. Mater. 55 (1997) 39–60.
[8] S.V. Ho, C.J. Athmer, P.W. Sheridan, B.M. Hughes, R. Orth, D. McKenzie, P.H. Brodsky, A. Shapiro, R. Thornton, J. Salvo, D. Schultz, R. Landis, R. Griffith, S. Shoemaker, The Lasagna technology for in situ soil remediation. 1. Small field test, Environ. Sci. Technol. 33 (1999) 1086–1091.
[9] Z.H. Li, I. Neretnieks, Electroremediation: removal of heavy metals from soils by using cation-selective membrane, Environ. Sci. Technol. 32 (1998) 394–397.
[10] A.B. Cundy, L. Hopkinson, Electrokinetic iron pan generation in unconsolidated sediments: implications for contaminated land remediation and soil engineering, Appl. Geochem. 20 (2005) 841–848.
[11] S. Habibi, A new electrokinetic technology for revitalization of oily sludge, Ph.D. Thesis, The Department of Building, Civil, and Environmental Engineering, Concordia University, Que., Canada, 2004.
[12] Standard Methods for the Examination of Water and Wastewater, 20th ed., American Public Health Association, American Water Works Association and Water Environment Federation, 1998, pp. 5–35 and 5–39.
[13] J. Guan, R. Amal, T.D. Waite, Effect of aggregate size and structure on specific resistance of biosolids filter cakes, Water Sci. Technol. 44 (2001) 215–220.
[14] http://www.grow.arizona.edu/water/waterscience/watermolecule.shtml.
[15] http://www.lsbu.ac.uk/water/molecule.html.
[16] http://www.engr.uga.edu/service/outreach/Final%20Biofuel%20Oil%20Report%20-%20Section%202%20Analysis%20of%20Fats%20and%20Grease.pdf.
[17] http://www.vegburner.co.uk/oils.htm.
[18] L.R. Droste, Theory and practice of water and wastewater treatment, John Wiley & Sons Inc., New York, 1997.
[19] L.L. Schramm, The influence of interfacial tension in the hot-water process for recovering bitumen from the Athabasca oil sands, Canadian International Petroleum Conference, Calgary, 2001, paper 2001–136.
[20] E. Mohamedelhassan, J.Q. Shang, Effect of electrode materials and current intermittence in electroosmosis, Ground Improv. 5 (2001) 3–11.
[21] N.V. Churaev, V.D. Sobolev, A.N. Zorin, Measurement of viscosity of liquids in quartz capillaries, in: Thin Liquid Films and Boundary Layers, Academic Press, New York, 1970.
[22] D.R. Crow, Principles and Applications of Electrochemistry, fourth ed., Blackie Academic and Professional, an imprint of Chapman & Hall, New York, 1994.
[23] http://global.horiba.com/story_e/conductivity/conductivity_04.htm.
[24] S.T. Wang, T. Chen, Momentum, Heat and Mass Transfer, second ed., Tianjin Science and Technology Press, Tianjin, China, 1988.